Neurobiology of Disease 191 (2024) 106387

Contents lists available at ScienceDirect

Neurobiology of Disease

journal homepage: www.elsevier.com/locate/ynbdi

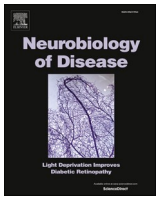

The mitochondriogenic but not the immunosuppressant effects of mTOR inhibitors prompt neuroprotection and delay disease evolution in a mouse model of progressive multiple sclerosis

Daniela Buonvicino [a,*], Sara Pratesi [b,1], Giuseppe Ranieri [a,1], Alessandra Pistolesi [a], Daniele Guasti [c], Alberto Chiarugi [a]

[a] Department of Health Sciences, Section of Clinical Pharmacology and Oncology, University of Florence, Florence, Italy
[b] Centre of Immunological Research DENOTHE, Department of Experimental and Clinical Medicine, University of Florence, Florence, Italy
[c] Department of Clinical and Experimental Medicine, Research Unit of Histology & Embryology, University of Florence, Florence, Italy

ARTICLE INFO

Keywords:
Progressive EAE
Dexamethasone
Fingolimod
Rapamycin
Mitochondria

ABSTRACT

Introduction: Purportedly, the progression of multiple sclerosis (MS) occurs when neurodegenerative processes due to derangement of axonal bioenergetics take over the autoimmune response. However, a clear picture of the causative interrelationship between autoimmunity and axonal mitochondrial dysfunction in progressive MS (PMS) pathogenesis waits to be provided.

Methods: In the present study, by adopting the NOD mouse model of PMS, we compared the pharmacological effects of the immunosuppressants dexamethasone and fingolimod with those of mTOR inhibitors rapamycin and everolimus that, in addition to immunosuppression, also regulate mitochondrial functioning. Female Non-Obese Diabetic (NOD) mice were immunized with MOG35–55 and treated with drugs to evaluate functional, immune and mitochondrial parameters during disease evolution.

Results: We found that dexamethasone and fingolimod did not affect the pattern of progression as well as survival. Conversely, mTOR inhibitors rapamycin and everolimus delayed disease progression and robustly extended survival of immunized mice. The same effects were obtained when treatment was delayed by 30 days after immunization. Remarkably, dexamethasone and fingolimod prompted the same degree of immunosuppression of rapamycin within both spleen and spinal cord of mice. However, only rapamycin prompted mitochondriogenesis by increasing mitochondrial content, and expression of several mitochondrial respiratory complex subunits, thereby preventing mtDNA reduction in the spinal cords of immunized mice. These pharmacodynamic effects were not reproduced in healthy NOD mice, suggesting a disease context-dependent pharmacodynamic effect.

Discussion: Data corroborate the key role of mitochondriogenesis to treatment of MS progression, and for the first time disclose the translational potential of mTOR inhibitors in PMS therapy.

1. Introduction

In spite of the recent approval of ocrelizumab and siponimod for the treatment of progressive multiple sclerosis (PMS), patients affected by this devastating disorder are still in great need of drugs able to suppress disease evolution. There is a large consensus that the difficulties in developing such remedies are mainly due to the still obscure etiopathogenesis of MS progression. In particular, whether and how immunopathology contributes to the cellular and molecular mechanisms underpinning neurodegeneration within the CNS of PMS patients remains to be clarified. Among the multiple hypotheses put forward, it has been proposed that axonopathy and ensuing neuronal cell death during

Abbreviations: Dex, dexamethasone; MOG, myelin oligodendrocyte glycoprotein; mt, mitochondrial; NOD, Non-obese diabetic; PEAE, progressive experimental autoimmune encephalomyelitis; PMS, progressive multiple sclerosis; Rapa, rapamycin..

* Corresponding author at: Department of Health Sciences, Section of Clinical Pharmacology and Oncology, University of Florence, Viale Pieraccini 6, Firenze 50139, Italy.
E-mail address: daniela.buonvicino@unifi.it (D. Buonvicino).

[1] These authors equally contributed to the study

https://doi.org/10.1016/j.nbd.2023.106387
Received 26 April 2023; Received in revised form 4 October 2023; Accepted 17 December 2023
Available online 22 December 2023

PMS are prompted by a state of virtual hypoxia within demyelinated axons secondary to mitochondrial inability to face increased ATP consumption due to intra-axonal derangement of ion homeostasis. This, in turn, triggers bioenergetic derangement, irreversible axonopathy and retrograde neuronal death (Sedel et al., 2016; Trapp and Stys, 2009). In this light, pharmacological approaches aimed at sustaining mitochondrial energy dynamics within the central nervous system (CNS) of PMS patients may represent a valid strategy to counteract disease progression (Armstrong, 2007; Campbell et al., 2019).

Recently, we characterized from a neuro- and immunopathological perspective the progressive experimental autoimmune encephalomyelitis (PEAE) in NOD mice as an animal model reminiscent of PMS (Buonvicino et al., 2019). In these mice, we investigated the effects of drugs that have an intrinsic translational potential to expedite a possible use in PMS therapy. Further, instead of partially analyzing the drugs' effects during the initial phase of progression, we planned to analyze how the various treatments impact the entire duration of disease evolution (about 6 months). We mainly focused on immunomodulatory as well as bioenergetics-boosting drugs. In keeping with the general insensitivity of PMS to immunosuppressive drugs, we found that experimental treatments with corticosteroids (Buonvicino et al., 2019) {Buonvicino, 2019 #1} or histone deacetylase inhibitors (Buonvicino et al., 2021){Buonvicino, 2021 #22} were unable to affect PEAE evolution, in spite of evidence of efficient immunosuppression within the mouse CNS. As for the effects of drugs able to sustain neuronal bioenergetics, we found that two compounds able to support mitochondrial functioning such as the PPARα-activator bezafibrate and the carboxylase-cofactor biotin were also unable to delay EAE progression in NOD mice (Buonvicino et al., 2019). Remarkably, however, dexpramipexole, the first-in-class activator of mitochondrial F_1F_o ATP synthase, significantly reduced the progression rate and prolonged survival of PEAE NOD mice (Buonvicino et al., 2020). These findings suggest that PEAE becomes independent from immune-mediated events during its evolution, being driven by derangement of energy dynamics that, in turn, sustain neurodegeneration.

Given the potential relevance of PEAE in NOD mice to the understanding of PMS pathogenesis and identification of innovative treatments, we planned to further investigate the pharmacotherapeutic effects of immunomodulatory drugs on disease evolution in PEAE NOD mice. We reasoned that exposure to immunosuppressants starting on the day of immunization should maximize control of the initial autoimmune response, thereby disclosing the full relevance of autoimmunity to PEAE pathogenesis. We therefore planned to test the effects of the potent immunosuppressants endowed with different pharmacodynamics such as dexamethasone and the sphingosine-1-phosphate analog fingolimod. We also tested the effect of the mTOR-inhibitor rapamycin because of its original, dual ability to suppress immune responses and promote mitochondrial bioenergetics (Pan et al., 2012; Thomson et al., 2009).

2. Methods

2.1. Animals

All animal care and experimental procedures were performed according to the European Community guidelines for animal care (European Communities Council Directive 2010/63/EU) and were approved by the Committee for Animal Care and Experimental Use of the University of Florence. Experimental autoimmune encephalomyelitis (EAE) is the most widely accepted animal model of multiple sclerosis (MS) (Mix et al., 2010). Given the well-known 3:1 female:male ratio in MS patients, EAE is typically induced in female animals and indeed only female mice were used in our study. Female NOD/ShiLtj mice (Charles River, Milan, Italy) were housed in a conventional unit (5–6 per cage) with free access to food (Harlan Global Diet 2018, Harlan Laboratories, Udine, Italy) and water, environmental enrichments, and maintained on a 12h light/dark cycle at 21 °C room temperature.

2.2. MOG $_{35–55}$ immunization and neuroscore evaluation

EAE was induced in 10-week-old NOD/ShiLtj mice with $MOG_{35–55}$ peptide (MEVGWYRSPFSRVVHLYRNGK) (synthesized by EspiKem Srl., University of Florence, Italy) (Buonvicino et al., 2019). Briefly, EAE was induced in each mouse by subcutaneous immunization with 300 μl: 100 μl in each flank and 100 μl at the base of the tail. The emulsion for each mouse is prepared as reported: 250 μg of $MOG_{35–55}$ peptide was solubilized in 150 μl of PBS, and this volume was emulsified in 150 μl complete Freund's adjuvant (Sigma, Milan, Italy) supplemented with 4 mg/ml of Mycobacterium-tuberculosis (strain H37Ra; Difco Laboratories, Detroit, Michigan, USA). The total volume was vortexed thoroughly for 1 h at 4 °C. Immediately thereafter and 48 h later, mice received i.p. injections of 200 ng Pertussis Toxin (Sigma, Milan, Italy) in 100 μl PBS. Then mice were randomized (generating groups by the RAND function of Excel software) and treated with dexamethasone, fingolimod, rapamycin, everolimus, SR18292 or vehicle as follows. Dexamethasone and fingolimod (Sigma, Milan, Italy) were dissolved in PBS and administrated per os on a daily basis at 0.3 $mg{\cdot}kg^{-1}$ body weight. Rapamycin and everolimus (Sigma, Milan, Italy) were dissolved in PBS and administrated per os on a daily basis at 1 $mg{\cdot}kg^{-1}$ body weight. SR18292 (Sigma, Milan, Italy) was dissolved in PBS administrated per os on a daily basis at 1 mg·kg − 1 body weight. Immunized vehicle-treated animals daily received the same amount of PBS. Treatments started on the day of immunization unless otherwise specified in the text. Clinical signs of EAE were examined every two days by blinded operators as reported (Buonvicino et al., 2019). The following score was assigned: 0, normal; 0.25 or 0.5, splay reflex test (performed by lifting the mouse by its tail and observing the degree of hindlimb splay during 10 s. If both hindlimbs were splayed outward away from the abdomen, a 0 score was assigned. If one or both hindlimbs were partially retracted toward the abdomen without touching it, a score of 0.25 or 0.5 was assigned, respectively); 1, weakness of the tail/hind limbs; 2, ataxia and/or difficulty in righting; 3, paralysis of the hind limbs and/or paresis of the forelimbs; 4, tetraplegia. When mice reached score 2, food and water were positioned on the floor of the cage for easy access. Because of ethical reasons, score 4 mice were euthanized as soon as they reached the score. Mice were euthanized by cervical dislocation after sedation with isoflurane. After the experiment conclusion, to evaluate the confirmed disability progression parameter we examined the neurological score of each single mouse. We then analyzed the score using a 4-day interval: whenever the score worsened for three consecutive data points, the day related to the first of the three data points was selected as a confirmed disability progression point. Two experiments with 8 mice/group were conducted. The group size was obtained with effect size d = 1.4 (Rothhammer et al., 2017), α error prob. = 0.05 and power = 0.8 by G*Power Version 3.0.10 (Franz Faul, University of Kiel, Germany).

2.3. Histological analysis

Histological analysis has been performed on control mice or mice that were immunized and randomized to identify vehicle-, rapamycin-, dexamethasone- and fingolimod-treated mice (5 mice/group). Lumbosacral spinal cords were collected from 120 post-immunization MOG-immunized NOD mice, fixed in 4% paraformaldehyde in 0.1-M PBS, embedded in paraffin and cut into 10-μm thin sections. The axonal loss was assessed by Bielschowsky's silver staining. For each spinal cord, serial sections of the lumbosacral portion have been collected at a 1-mm interval and distributed onto slides for a total of five sections per slide. Images were acquired by using an Olympus BX40 microscope (Olympus, Milan, Italy) and a digital camera (Olympus DP50) with NIS-Elements software (NIS-Elements); sections were analyzed by a blinded operator by using ImageJ software (ImageJ) (Buonvicino et al., 2019).

2.4. Flow cytometry

Spinal cord infiltrating leukocytes were characterized by flow cytometry. Briefly, control mice (10-week old NOD mice) or MOG-immunized NOD mice (5 mice/group) were sacrificed at day 30 post-immunization and perfused with cold saline before organ collection. Then a single-cell suspension for each sample was prepared and stained with anti-CD4 FITC and anti-CD8 PE or isotype-matched control IgG antibodies (all from Miltenyi Biotec, Bergisch Gladbach, Germany) according to the manufacturer's instructions. The cells were then analyzed using a FACSCanto II flow cytometer (BD Biosciences) equipped with FACSDiva software (BD Biosciences), acquiring a total of 10^5 events for each spinal cord extract (Cavone et al., 2015).

2.5. Lymphocyte proliferation and ELISA

Mononuclear cells extracted from the spleen of control, $MOG_{35–55}$-immunized mice treated or not for 30 days with dexamethasone (0.3 $mg{\cdot}kg^{-1}$ per os, daily), fingolimod (0.3 $mg{\cdot}kg^{-1}$ per os, daily) or rapamycin (1 $mg{\cdot}kg^{-1}$ per os, daily) (5 mice/group) were cultured in complete RPMI (Life Technologies, Monza, Italy) in 96 wells plates (2×10^5 cells per well) and re-challenged or not with $MOG_{35–55}$ (20 μg/ml). After 72 h, the proliferative response was measured by [^{3}H]thymidine (Perkin Elmer, Milan, Italy) incorporation as reported (Cavone et al., 2015). Supernatants were collected after 72 h of culture for IFNγ measurements by ELISA (Life Technologies, Monza, Italy) according to the manufacturer's instructions. The detection limit for IFNγ is 5.3 pg/ml.

2.6. Immunohistochemistry

For immunohistochemical analysis, lumbosacral spinal cords from control or MOG-immunized NOD mice, treated with vehicle, rapamycin, fingolimod or dexamethasone from day 1 to day 30 after immunization, were collected; 10-μm thin sections were blocked with 5% normal goat serum (Thermo Fisher Scientific, Waltham, MA, USA) containing 0.3% Triton X-100 (Sigma, Milan, Italy). One hour later, sections were incubated overnight at 4 °C with a rabbit polyclonal anti-ionized calcium-binding adapter molecule 1 (IBA1) (1:300, Wako Cat# 013–26,471, RRID: AB_2687911) for microglia, or with a chicken polyclonal antibodies against the glial fibrillary acidic protein (GFAP) (1:500, Synaptic System Cat# 173006). After washings, sections were incubated with an anti-rabbit secondary antibody conjugated with AlexaFluor 546 (1:2000, (Thermo Fisher Scientific Cat# A-11035) or with an anti-Chicken secondary antibody, Alexa Fluor™ 488 (1:1000, Thermo Fisher Cat# A-11039). Images were acquired under a LEICA TCS SP5 confocal laser scanning microscope (Leica Microsystems CMS GmbH, Mannheim, Germany) with a 20× objective. Quantification of astrocytes and microglia immunofluorescence was performed using ImageJ. Values correspond to the mean of four different microscopic fields of five different mouse spinal cord sections. The analysis was conducted on 5 mice per group.

2.7. Quantitative PCR

Genomic DNA was extracted from mice spinal cords with the NucleoSpin TriPrep kit (Macherey-Nagel, Duren, Germany). Mitochondrial content was quantified by measuring the ratio between the mitochondrial *Nd1* and nuclear *β-actin* gene amplification products as reported (Felici et al., 2017). The following primers were used: *mt-Nd1* forward 5'-TGCCAGCCTGACCCATAGCCATA-3′ and reverse 5'-ATTCTCCTTCTGTCAGGTCGAAGGG-3′; *β-actin* forward 5'-GCAGCCACATTCCCGCGGTGTAG-3′ and reverse 5'-CCGGTTTGGACAAAGACCCAGAGG-3′.

Total RNA was isolated from the spleen and spinal cords of control or NOD-immunized mice using Trizol Reagent (Life Technologies, Monza, Italy). One μg of RNA was retrotranscribed using iScript (Bio-Rad, Milan, Italy). RT-PCR was performed as reported (Buonvicino et al., 2018). The following primers were used: *T-bet*: forward 5′- TGCCTACCAGAACGCAGAGATCACTC -3′ and reverse 5'-GTAGAAACGGCTGGGAACAGGATACTG −3′; *RORγt*: forward 5′- CCATTCAGTATGTGGTG GAGTTTGCCAA −3′ and reverse 5′- GCAGCCCAAGGCTCGAAACAGCT -3′; GATA3: forward 5′-TGCCTGTGGGCTGTACTACAAGCTTCA-3′ and reverse 5′-GATGTGGCTCAGGGATGACATGTGTC-3′; IL10: forward 5′-GGGTTGCCAAGCCTTATCGGAAATGA-3′ and reverse 5′-CACTCTTCACCTGCTCCACTGCC-3′; IFNγ: forward 5′- TCAGGCCATCAGCAACAACATAAGCG −3′ and reverse 5′- TTCCGCTTCCTGAGGCTGGATTCC -3′; Foxp3: forward 5′-CAAGCAGATCATCTCCTGGAT-3′ and reverse 5′-GTGGCTACGATGCAGCAAGAG-3′; PGC1-α: forward 5′-GACAGATGGAG CCGTGACCACTG-3′ and reverse 5′-CTGATCCTGTGGGTGTGGTTTGC-3; mt-Nd2 forward 5'-ATTATCCTCCTGGCCATCGTA-3′ and reverse 5'-AAGTCCTATGTGCAGTGGGAT-3′; Ndufv2 forward 5'-GTGCACAAT GGTGCTGGAGGAG-3′ and reverse 5'-GGTAGCCATCCATTCTGCC TTTGG-3′; Atp5d forward 5'-CAGCACGGGCTGAGATCCAGAT-3′ and reverse 5'-GACAGGCACCAGGAAGCTTTAAGC-3′; Cox1 forward 5′-TATCAATGGGAGCAGTGTTTG-3′ and reverse 5′-AGGCCCAGGAAAT GTTGAG-3' 18S forward 5'-AAAACCAACCCGGTGAGCTCCCTC-3′ and reverse 5'-CTCAGGCTCCCTCTCCGGAATCG-3′. Primers were purchased from Integrated DNA Technologies (Iowa, USA). Primers were purchased from Integrated DNA Technologies (Iowa, USA). The analysis was conducted on 5 mice per group unless otherwise specified in the text.

2.8. Transmission electron microscopy

Transmission electron microscopy was performed as previously described (Felici et al., 2017). Briefly, the spinal cord was fixed in Karnovsky's solution, post-fixed in 1% osmium tetroxide and embedded in Epon 812. Ultrathin sections were stained with uranyl acetate and alkaline bismuth subnitrate and examined under a JEM 1010 electron microscope (Jeol, Tokyo, Japan) at 80 kV. Micrographs were taken at final magnifications of 12,000× and 80,000× using a MegaView III digital camera and interfacing software (SIS-Soft Imaging System, Munster, Germany). The mitochondrial area was calculated in each image at a magnification of 80,000×. To analyze the cristae area, only mitochondria unequivocally present within axoplasmic fields were analyzed. Areas of cristae and mitochondria were measured using iTEM image analysis software (SIS). The analysis was conducted on 5 mice per group.

2.9. Western blot

Lumbar spinal cord tissue was dissolved in 1% SDS. BCA (bicinchoninic acid) Protein Assay was used to quantify the total protein levels. Lysates (20 μg/lane of protein) were resolved by electrophoresis on a 4–20% SDS-polyacrylamide gel (Bio-Rad Laboratories, Hercules, CA, USA) and transferred onto nitrocellulose membranes. After blocking, the blots were incubated overnight at 4 °C with VDAC1 (ab14734 from Abcam, Cambridge, London, UK) or Phospho-p70 S6 Kinase (Thr389) (Ab #9234 from Cell signaling, Massachusetts, USA) in TBS-T containing 5% bovine serum albumin. Tubulin was used as a loading control (T9026, monoclonal antibody purchased from Sigma (St. Louis, MO, USA). Immunodetection was performed with HRP-conjugated secondary antibodies (diluted 1:2000 anti-mouse) (Amersham Biosciences, Little Chalfont, UK) in TBS-T containing 5% non-fat dry milk. After washing, the membranes were detected using chemiluminescence (ECL plus; Euroclone, Padova, Italy). Quantity One analysis software was used for quantitative analysis (Bio-Rad, Hercules, CA, USA). Results are presented as the mean standard error of the mean (SEM) of different gels and expressed as AU-, which depicts the ratio between levels of target protein expression and tubulin normalized to basal levels (Landucci et al., 2021). The analysis was conducted on 6 mice per group unless otherwise specified in the text.

2.10. Sample preparation and LC-MS/MS analysis

Whole blood and spinal cord samples were collected after 10 days of treatment with fingolimod (0.3 mg/kg) with oral or intraperitoneal administration (8 mice/group). The whole blood sample was collected by cardiac puncture immediately following euthanasia, and then the spinal cord was extracted. Frozen plasma and spinal cord samples were thawed at room temperature. A 10 μl aliquot of blood was transferred in a 1.5 ml Eppendorf tube and mixed with an internal standard (IS) solution 2-undecylpiperidine-3,4,5-triol (kindly synthesized by Prof. Cardona, Department of Chemistry, University of Florence) 1.5 μl of 10 ng/ul, 150 μl of 100 mM NaOH and 1 ml of tertbutylmethylether: dichloromethane solution (75:25, *v*/v). The sample was shaken at room temperature for 1 h and then centrifuged for 10 min at 12000 rpm in a refrigerated centrifuge (4 °C). The organic layer was recovered and dried under a nitrogen flow. The residue was solubilized in 50 μl of MeOH and transferred in an autosampler vial for LC-MS/MS analysis. Spinal cord homogenates were prepared in MeOH with 0.1% FoAc. After centrifugation, 10 μl were taken and mixed to the internal standard solution AGFCCF84 (1.5 μl of 10 ng/ul), 23.5 μl of ACN (containing 0.1% FoAc) and 75 μl of H_2O (containing 0.1% FoAc). The mixture was loaded on a Hybrid SPE cartridge and the eluate was immediately collected and then transferred in an autosampler vial for the LC-MS/MS analysis.

A Series 200 HPLC, equipped with an autosampler and column oven (Perkin Elmer, USA) coupled to a 4000 QTRAP mass spectrometer with TurboV ion spray interface was used (Sciex, Toronto, Canada). The LC column was a Synergy Fusion, 3 × 150 mm, 4 μm (Phenomenex, Torrance, CA, USA), maintained at 40 °C. The mobile phases were 10 mM AmAc with 0.1% FoAc (A) and MeOH with 0.1% FoAc (B). The gradient elution program started at 5% B, then linearly increased to 95% B in 4 min, maintained for 5 min; then the composition returned to the initial condition in 2 min and the column was re-equilibrated for 10 min, for a total run time of 21 min. The column flow rate was 0.4 ml/min. The MS parameters were optimized by infusing a solution of fingolimod and IS into the TurboV Ion spray interface, operating in positive ion mode. The $[M + H]^+$ ion was generated for the two molecules. Ion spray potential was 5.2 kV, temperature 520 °C, curtain gas, GS1 and GS2 gas were set at 30, 35 and 45, respectively. The gas was high purity N_2, used also as collision gas (CAD gas) set to medium (vacuum 3.3×10^{-5} Torr).

The MRM transitions and other analyte-dependent parameters are reported in Table 1. Two transitions were acquired for fingolimod and IS; a fifth transition was used to monitor the presence of main phospholipids (phosphatidylcholines) in biological samples using a generic 184 *m/z* to 184 m/z transition (choline head group ion).

The dwell time was 300 msec for each transition, excluding the last, which was 20 msec. Q 1 and Q 3 resolution was set to the unit. For data acquisition and analysis the Analyst software (ver.1.6.3) was used. A comparison of signal intensity of fingolimod in the different matrices (whole blood an spinal cord), normalizing it considering the response ratio to the internal standard (added in the same amount in all samples) was conducted. The relative abundance of fingolimod in the different matrices depending on the route of administration was reported.

2.11. Statistical analysis

The data and statistical analysis comply with the recommendations on experimental design and analysis in pharmacology (Curtis et al., 2018). Data are expressed as mean ± SEM. In order to evaluate the difference in continuous parameters between two groups, Mann-Whitney test (according to Kolmogorov-Smirnov test for normality and Bartlett's test for variance equality) is used. To test the difference in continuous parameters between more than two groups Kruskal-Wallis and post hoc Dunn's test (according to Kolmogorov-Smirnov test for normality and Bartlett's test for variance equality) are used. The differences in overall survival and confirmed disease progression between groups are tested using Kaplan-Meier curve and Log-rank test.

Differences were considered to be significant when p-value<0.05. Statistical analyses were carried out using GraphPad Prism (version 8).

3. Results

3.1. Effects of dexamethasone, fingolimod and rapamycin on PEAE in NOD mice

Prior work in NOD mice with PEAE mostly evaluated disease evolution for a short time, thereby providing incomplete information on progression features, and long-lasting effects of experimental treatments (Basso et al., 2008; Farez et al., 2009; Huntington et al., 2006; Ichikawa et al., 2000; Mayo et al., 2016). We, therefore, evaluated the disease course until each animal reached score 4, a time point approximately corresponding to 6 months after immunization. Further, to maximize the pharmacodynamic effects of immunosuppressants, we started treatments concomitantly to immunization. Drugs were administered orally, to be consistent with the use of a neurotherapeutic in a chronic disorder.

In good agreement with prior studies from our group (Buonvicino et al., 2019), all the NOD mice immunized with $MOG_{35–55}$ showed an inexorable progression of neurological disability up to score 4, and no sign of early or delayed remission. Remarkably, daily treatment with dexamethasone (0,3 $mg{\cdot}kg^{-1}$) from day 0 had no effects on key parameters of EAE progression such as disease onset, severity and duration (Fig. 1A). Mortality was also not affected in mice receiving dexamethasone (Fig. 1B). The lack of effects of preventive treatment with dexamethasone was surprising given the drug's ability to provide protection from RR-EAE in numerous mouse strains when administered at the day of immunization (Donia et al., 2010). Thus, to further characterize the effects of immunosuppressants on PEAE in NOD mice, we exposed the animals to the sphingosine 1 phosphate analog fingolimod. We chose this drug because of its unique ability to entrap lymphocytes in lymph nodes, thereby preventing CNS immune invasion (Colombo and Farina, 2021), a pharmacodynamic effect distinct from that of drugs directly targeting lymphocyte differentiation or immune activation. Again, the daily administration of fingolimod from the day of immunization showed no effects on the pattern of disease onset and evolution (Fig. 1C), as well as on survival (Fig. 1D) of NOD mice with PEAE. To gather additional information on the effect of immunosuppression on the progression of EAE in NOD mice, we exposed the animals to rapamycin, a potent suppressant of adaptive immunity routinely used to prevent graft rejection (Nguyen et al., 2019). We found that mice challenged with rapamycin starting from day 0 post-immunization showed an identical disease onset compared to those receiving vehicle, but a significantly reduced progression rate (Fig. 1E). In keeping with this, treatment with rapamycin reduced the mortality rate of PEAE NOD mice (Fig. 1F), with

Table 1
The MRM transitions and other analyte-dependent parameters for fingolimod, internal standard (IS) and phospholipids (PLs) are reported.

	Retention time (min)	Precursor ion (m/z)	Product ion (m/z)	DP (V)	EP (V)	CE (V)	CXP (V)
fingolimod	8.39	308.4	255.3 203.3	95	12	23 24.5	14.5 10.5
IS	8.67	316.3	238.3 212.3	45	10	30 30	9 9
PLs		184.0	184.0	125	10	5	15

median survival values of 138 and 198 days [HR = 2.280 (1016 to 5116), $p = 0.015$] in vehicle- and rapamycin-treated mice, respectively. A key parameter of disease evolution in PMS patients is 12-week confirmed disability progression. We therefore also attempted to evaluate this parameter in PEAE NOD mice using a 4-day interval. Of note, we found a significant difference in confirmed disability progression between vehicle and rapamycin-treated mice (Fig. 1G), with a reduction in the probability of progression showing a HR of 2276 (1034 to 5006), ($p = 0.011$). To strengthen our results obtained with rapamycin, we also tested everolimus, another mTOR inhibitor widely used in the clinic (Falkowski and Woillard, 2019; Rubin Suarez et al., 2017). We found that a daily administration of everolimus from the day of immunization showed a reduced progression rate and mortality rate of PEAE NOD mice (Supplementary Fig. 1 A and B). In particular, daily treatment with everolimus reduced mortality rate, with median survival values of 130 and 185 days [HR = 2.275 (0,954 to 5524), $p = 0.017$] in vehicle- and everolimus-treated mice, respectively. As regards the confirmed disability progression parameter, we did not find a significant difference between vehicle and everolimus-treated mice (Supplementary Fig. 1C). Notably, the two mTOR inhibitors tested at the same dose showed a similar effect on disease evolution, indeed both inhibitors did not alter disease onset but counteract disease progression.

Because of the unique ability of mTOR inhibitors to counteract disease evolution in PEAE NOD mice, we next investigated whether rapamycin affords protection even when tested in a clinically relevant, post-treatment protocol. Fig. 2A shows that a reduction of progression rate identical to that achieved in mice treated from day 0 post-immunization occurred even when drug exposure was delayed by 30 days. This treatment schedule also robustly reduced mortality rate, with median survival values of 136 and 200 days [HR = 2.890 (1199 to 6964), $p = 0.0019$] in vehicle- and rapamycin-treated mice, respectively. Likewise, treatment delayed confirmation of disability progression (HR of 2.538 (0,9588 to 6716), ($p = 0.018$) (Fig. 2B and C). In keeping with the ability of rapamycin to counteract disease evolution, by evaluating spinal cord neuropathology at day 120 from immunization, we found that daily treatment with rapamycin from the day after immunization significantly reduced the axonal loss in the lumbar spinal cord columns compared to those receiving the vehicle, dexamethasone or fingolimod (Fig. 3A and B).

3.2. Effects of rapamycin, fingolimod and dexamethasone on the adaptive and innate immunity in PEAE NOD mice

Taken together, data indicated that among the tested immunosuppressants, only rapamycin prompts qualitative or quantitative pharmacodynamic effects that suppress the autoimmune response and/or neurodegenerative component to an extent sufficient to counteract disease progression in PEAE NOD mice. Of course, the identification of the mechanisms underpinning these therapeutic effects might be of remarkable relevance to PMS therapy. Hence, in order to understand whether rapamycin affects the autoimmune response differently from dexamethasone or fingolimod, we evaluated the drugs' effects on multiple parameters of the immune response. Given that, in our previous paper (Buonvicino et al., 2019) we reported that immune parameters change during neurological score progression, we planned to evaluate the effect of these three drugs at an early time point. We selected 30 days after immunization, a time in which the neurological score was minimal, but the inflammatory processes were underway. We first analyzed the impact of the three immunosuppressants on sensitization to the myelin peptide. Fig. 4A shows that the proliferation of $MOG_{35–55}$-specific spleen lymphocytes was similarly reduced in mice treated with rapamycin, fingolimod and dexamethasone compared to vehicle-treated mice. In keeping with this, the reduced release of INFγ in the medium of $MOG_{35–55}$-exposed lymphocytes is similar for the three immunosuppressants compared to vehicle-treated mice (Supplementary Fig. 2 A). Accordingly, in the spleens of drugs-treated mice, we found a similar reduction of transcripts for Tbet and RORγt, markers of Th1 and Th17, respectively (Fig. 4B). Conversely, the three drugs did not change the unaltered transcript for GATA3 and FOXP3, markers of Th2 and Treg lymphocytes, respectively (Fig. 4B).

We also evaluated the spinal cord infiltrates and found that in keeping with data in the spleen, rapamycin, dexamethasone and fingolimod similarly reduced the number of CNS-invading lymphocytes. Specifically, the three immunosuppressants completely prevented $MOG_{35–55}$-dependent $CD4^+$ T cell infiltration, whereas only reduced that of $CD8^+$ lymphocytes (Fig. 4C). Consistent with the abrogation of $CD4^+$ cell migration, the increase of spinal cord mRNA levels for $Tbet^+$ —Th1 and $ROR\gamma t^+$ —Th17, and their cytokines IFNγ and IL-17, was also reduced to control levels in animals challenged with the immunosuppressants (Fig. 4D and Supplementary Fig. 2B and C). Conversely, the treatment with the three drugs did not alter spleen and spinal cord transcripts for the Th2 cell marker GATA3 or the Treg marker Foxp3 (Fig. 4B and D). We also asked whether fingolimod was able to exert its lymphocyte-entrapping ability in lymph nodes of immunized NOD mice. We, therefore, analyzed the volume of draining lymph nodes of the animals at day 30 post-immunization and found a dramatic increase in those exposed to fingolimod (Fig. 4E and F). Accordingly, a cytofluorimetric analysis of draining lymph nodes revealed a significant increase of $CD3^+$ cells after treatment with fingolimod compared to vehicle (Fig. 4G). In contrast with our data on the inability of fingolimod to counteract disease evolution, prior work shows that fingolimod affords protection from EAE in NOD mice adopting a daily dose identical to that we used (0.3 mg·kg − 1) but a 40-day i.p. post-treatment (Rothhammer et al., 2017). To rule out that this difference could be due to the route of administration, we compared the relative quantitation of fingolimod in the blood and spinal cord after oral and intraperitoneal routes at a dose of 0.3 mg/kg. Notably, we found that 10 days of treatment induced a 10-fold increase in drug blood and spinal cord contents when administered orally compared to intraperitoneally (Fig. 4H).

In light of the pathogenetic role of innate immunity in neurodegeneration during MS progression (Wang et al., 2019), and the potential effects of the three immunosuppressants on this immune component, we also evaluated the effect of rapamycin, fingolimod, and dexamethasone on microglia and astrocyte activation. We found that 30 days of immunization induced an astrocyte and microglia activation within the spinal cord and that, to a similar extent, 30 days of treatment with every one of the three drugs reduced the microglial activation, whilst a non-significative trend to reduction in astrocyte activation could be observed (Fig. 5 A-D).

These findings taken together indicated that the therapeutic effects of rapamycin in PEAE NOD mice could not be ascribed to a degree of immunosuppression more pronounced than the one prompted by fingolimod or dexamethasone.

3.3. Effects of rapamycin, fingolimod, and dexamethasone on mitochondrial homeostasis in PEAE NOD mice

Among the pleiotropic pharmacodynamic effects of rapamycin, a large body of evidence demonstrates that the drug promotes mitochondrial bioenergetics, thereby sustaining neuronal energy dynamics and survival (Ferese et al., 2020; Johnson et al., 2013; Zheng et al., 2016). Because of the pathogenetic role of mitochondrial dysfunction in MS pathogenesis (Campbell and Mahad, 2018; Witte et al., 2014) and, in particular, disease progression (Campbell et al., 2019), we next wondered whether rapamycin affected mitochondrial homeostasis in the spinal cord of PEAE NOD mice. As well as immune parameters, in our previous paper (Buonvicino et al., 2019) we reported that also mitochondrial parameters change during neurological score progression, to evaluate the effect of rapamycin we selected 30 days after immunization, a time in which the neurological score was minimal, but the inflammatory processes were underway. We first evaluated

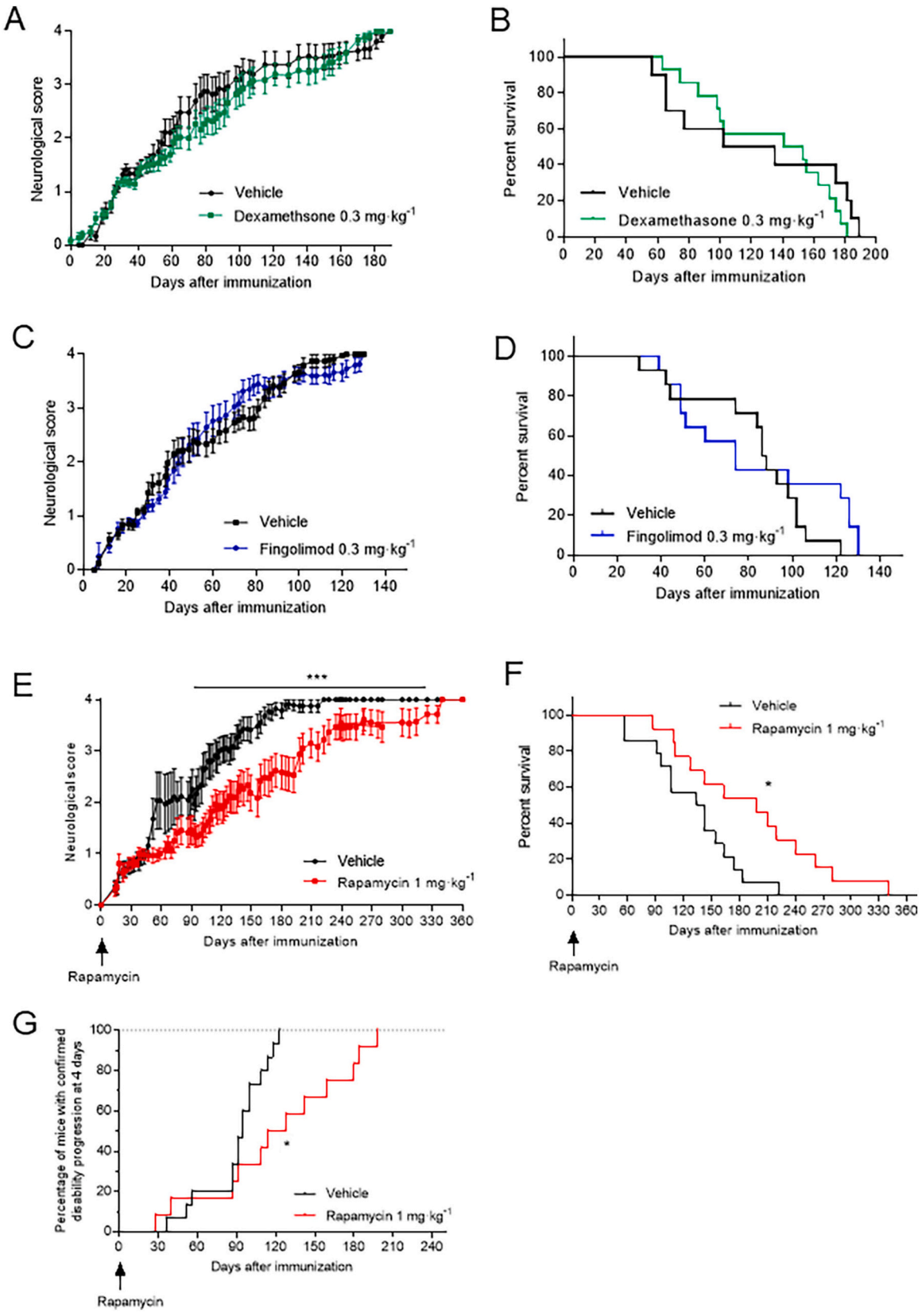

Fig. 1. Effects of dexamethasone, fingolimod, and rapamycin on disease progression and survival in PPEAE NOD mice. Effects of daily, oral treatment with dexamethasone (0.3 mg·kg^{-1}), fingolimod (0.3 mg·kg^{-1}) and rapamycin (1 mg·kg^{-1}) from the day of immunization on neurological score (A, C, and E, respectively) and survival (B, D, and F, respectively) in $MOG_{35–55}$- immunized NOD mice. Effects of daily, oral treatment with rapamycin (1 mg·kg − 1, daily from the day of immunization) on confirmed disability progression (G) in $MOG_{35–55}$- immunized NOD mice ($n = 16$ mice per group; Mann Whitney test and Long-rank test). *$p <$ 0.05, ***$p < 0.001$ vs Vehicle.

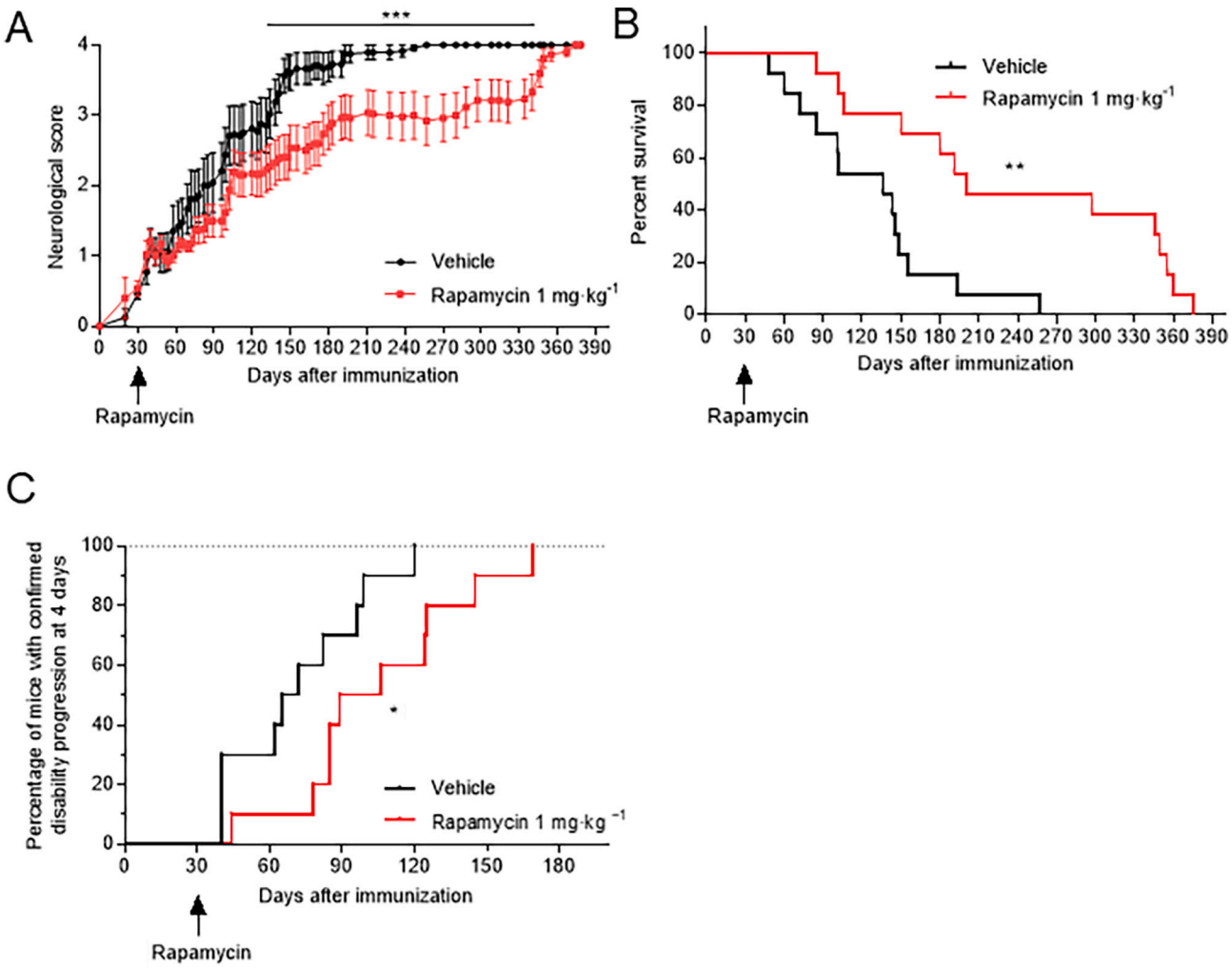

Fig. 2. Effects of rapamycin administered after disease onset on disease progression and survival in PPEAE NOD mice. Effects of daily, oral treatment with rapamycin (1 mg·kg^{-1}, daily from day 30 post-immunization) on (A) neurological score, (B) survival and (C) confirmed disability progression in $MOG_{35–55}$- immunized NOD mice (n = 16 mice per group; Mann Whitney test and Long-rank test). *p < 0.05, **p < 0.01, ***p < 0.001 vs Vehicle.

phosphorylation levels of S6K, a kinase directly phosphorylated by the rapamycin target mTORC1. In keeping with the ability of rapamycin to inhibit mTORC1 kinase activity, phospho-S6K levels were reduced in the lumbar spinal cord of PEAE NOD mice exposed (30 days) to the drug compared to phosphorylation levels found in animals receiving vehicle (Fig. 6A and B). Prior work reported that mtDNA levels, a prototypical index of tissue mitochondrial content, are reduced at early time points (neuroscore 1) in the spinal cord of PEAE NOD mice (Buonvicino et al., 2019). Because of the ability of rapamycin to promote expression of the mitochondrial master regulator PGC1α and mitochondriogenesis, we wondered whether the drug was able to increase PGC1α transcript levels and counteract mtDNA depletion in PEAE mice. Indeed, we found that treatment with rapamycin increased spinal cord expression of PGC1α (Fig. 6C), as well as mtDNA content (Fig. 6D). In keeping with this, we found that the number of axonal mitochondria increased in the spinal cord of rapamycin-treated mice NOD compared to vehicle mice (Fig. 6E and F). Accordingly, rapamycin treatment increased spinal cord expression levels of Voltage-dependent anion channel (VDAC), a proteomic marker of cellular mitochondrial content (Fig. 6G and H). In light of the impact of rapamycin on mitochondrial homeostasis of PEAE mice, and also to gather additional information on how the drug affected bioenergetic parameters within the CNS of these animals, we next evaluated expression levels of several mitochondrial respiratory complex subunits in their spinal cords. Fig. 6I shows that the drug almost doubled the transcripts of all the respiratory subunits evaluated except for ND2. Together, these findings prompted us to evaluate mitochondrial morphology within axons of spinal cord lateral columns, a region undergoing massive degeneration during the late stages of EAE progression in NOD mice (Buonvicino et al., 2019). By means of electron microscopy and analysis of hundreds of microscopic fields (see methods), we first evaluated the mitochondrial area and found no difference in PEAE mice exposed or not to rapamycin (Fig. 6J). Similarly, treatment with rapamycin did not affect the mitochondrial cristae area (Fig. 6K and L). To evaluate the correlation between PGC1α, mitochondriogenesis, and neuroprotective effects of rapamycin, we performed an experiment in which immunized NOD mice received a co-treatment from the day after immunization with rapamycin and a PGC1a inhibitor, the SR18292 (Raggi et al., 2021; Sharabi et al., 2017). We found that the treatment with SR18292 did not alter the neuroprotective effect of rapamycin (Fig. 6M), suggesting that PGC1α reasonably was not the only transcriptional coactivator responsible for rapamycin-induced mitochondriogenesis and neuroprotective effects.

We also evaluated whether dexamethasone or fingolimod similarly affected mitochondrial homeostasis in the spinal cord of PEAE mice. We found that at variance with rapamycin, the two drugs were unable to increase mtDNA content (Fig. 7A), VDAC expression (Fig. 7B and C) and mitochondrial number (Fig. 7D and E), as well as transcript levels of respiratory complex subunits (Fig. 7F). Further, neither dexamethasone

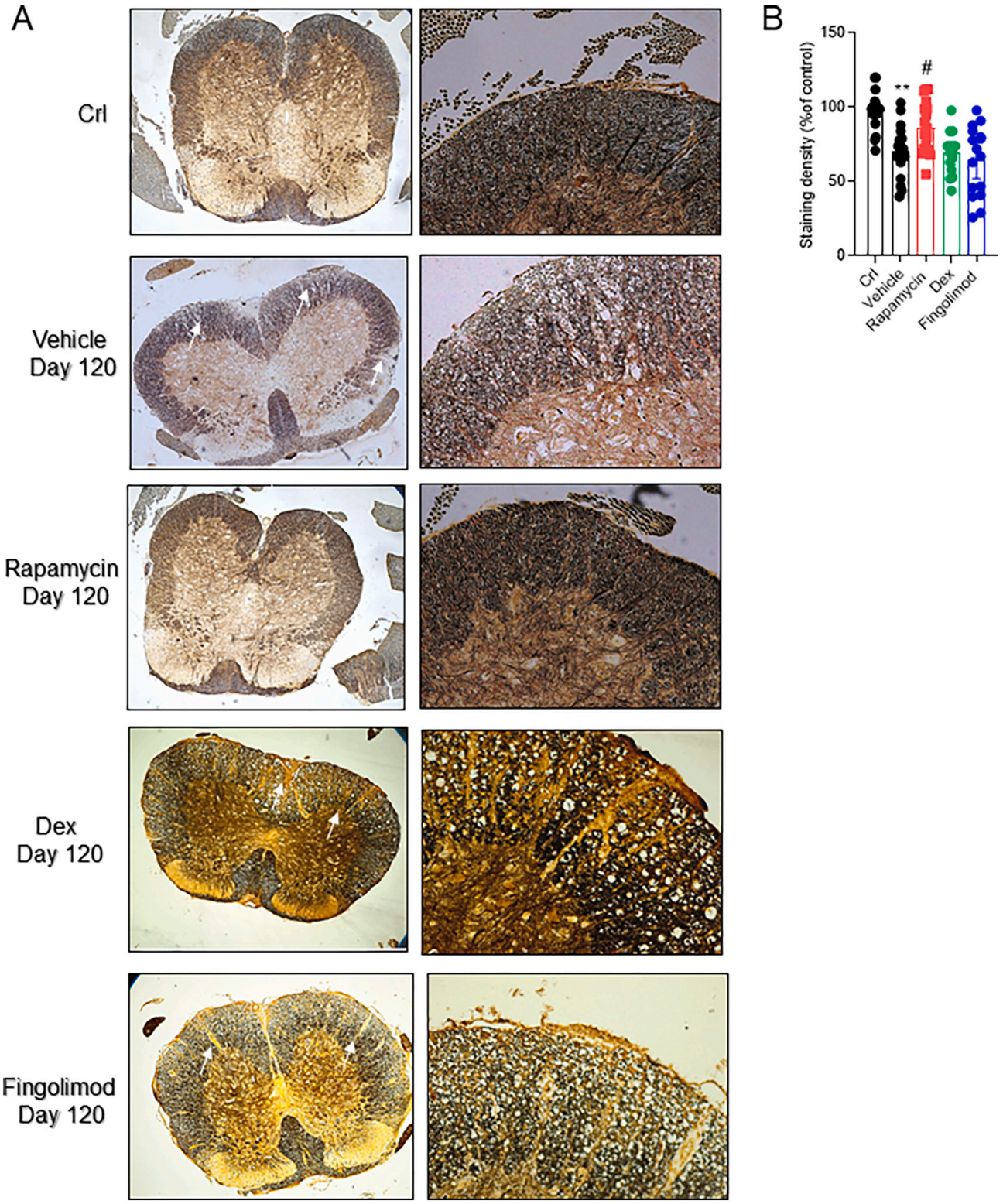

Fig. 3. Effects of rapamycin, dexamethasone and fingolimod on neurodegeneration in the spinal cord of PPEAE NOD mice. Visualization (4× and 20×) (A) and quantitation (B) of Bielschowsky stained spinal cord sections of control or MOG_{35-55}-immunized NOD mice at day 120 post-immunization treated with vehicle, rapamycin (1 mg·kg^{-1} per os), dexamethasone (0.3 mg·kg^{-1} per os) or fingolimod (0.3 mg·kg^{-1} per os) from the day of immunization. In (B), each column is the mean ± SEM of five mice per group, four sections per mouse (ANOVA plus Tukey's test).**$p < 0.01$ vs Crl, #$p < 0.05$ vs Vehicle.

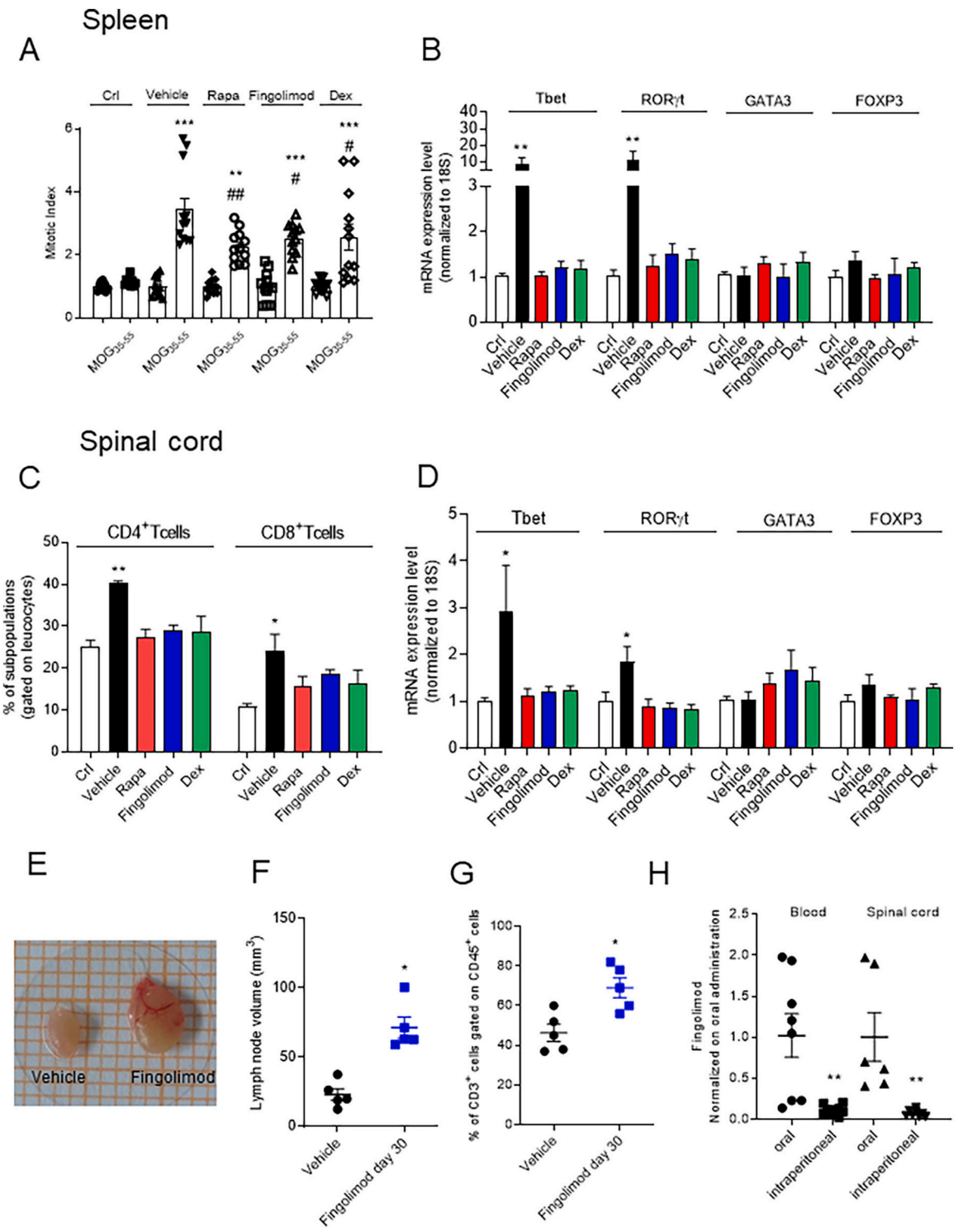

Fig. 4. Effects of rapamycin, dexamethasone and fingolimod on adaptive immunity in PPEAE NOD mice. Effects of daily oral treatment (from day 0 to 30 post-immunization) with rapamycin (1 mg·kg^{-1}), dexamethasone (0.3 mg·kg^{-1}) and fingolimod (0.3 mg·kg^{-1}) on spleen lymphocytes proliferation harvested from day 30 MOG_{35-55}-immunized NOD mice and re-challenged in vitro with MOG_{35-55} (20 μg/ml) (A). Effects of daily treatment with rapamycin, dexamethasone or fingolimod on the expression of T bet+-Th1, RORyt+-Th17, GATA3 + -Th2 and FOXP3 + -Treg in the spleen of control, vehicle- or drugs-treated NOD mice at day 30 after immunization (B). Effects of daily treatment from day 0 to 30 post-immunization with rapamycin, dexamethasone and fingolimod on FACS analysis of CD4 and CD8 positive cells (C) and the expression of T bet+-Th1, RORyt+-Th17, GATA3 + -Th2 and FOXP3 + -Treg (D) in the spinal cord of control, vehicle- or drugs-treated NOD mice. Effects of daily treatment from day 0 to 30 post-immunization with vehicle or fingolimod (0.3 mg·kg^{-1}, daily) on representative (E) and quantitative volume (F) of inguinal lymph nodes, and on FACS analysis of CD3 positive cells gated on CD45 positive cells (G) in the draining lymph nodes of NOD mice. Relative abundance of fingolimod measured in the whole blood and spinal cord of NOD mice treated orally or intraperitoneally with 0.3 mg kg − 1 fingolimod for 10 days (H). Each column (A-D) is the mean ± SEM of at least 5 animals per group. *p < 0.05, **p < 0.01, ***p < 0.001 vs Crl, #p < 0.05, ## p < 0.01 vs Vehicle, ANOVA plus Tukey's test. Each column (F—H) is the mean ± SEM of 5 animals per group. *p < 0.05 vs Vehicle, Student's *t*-test.

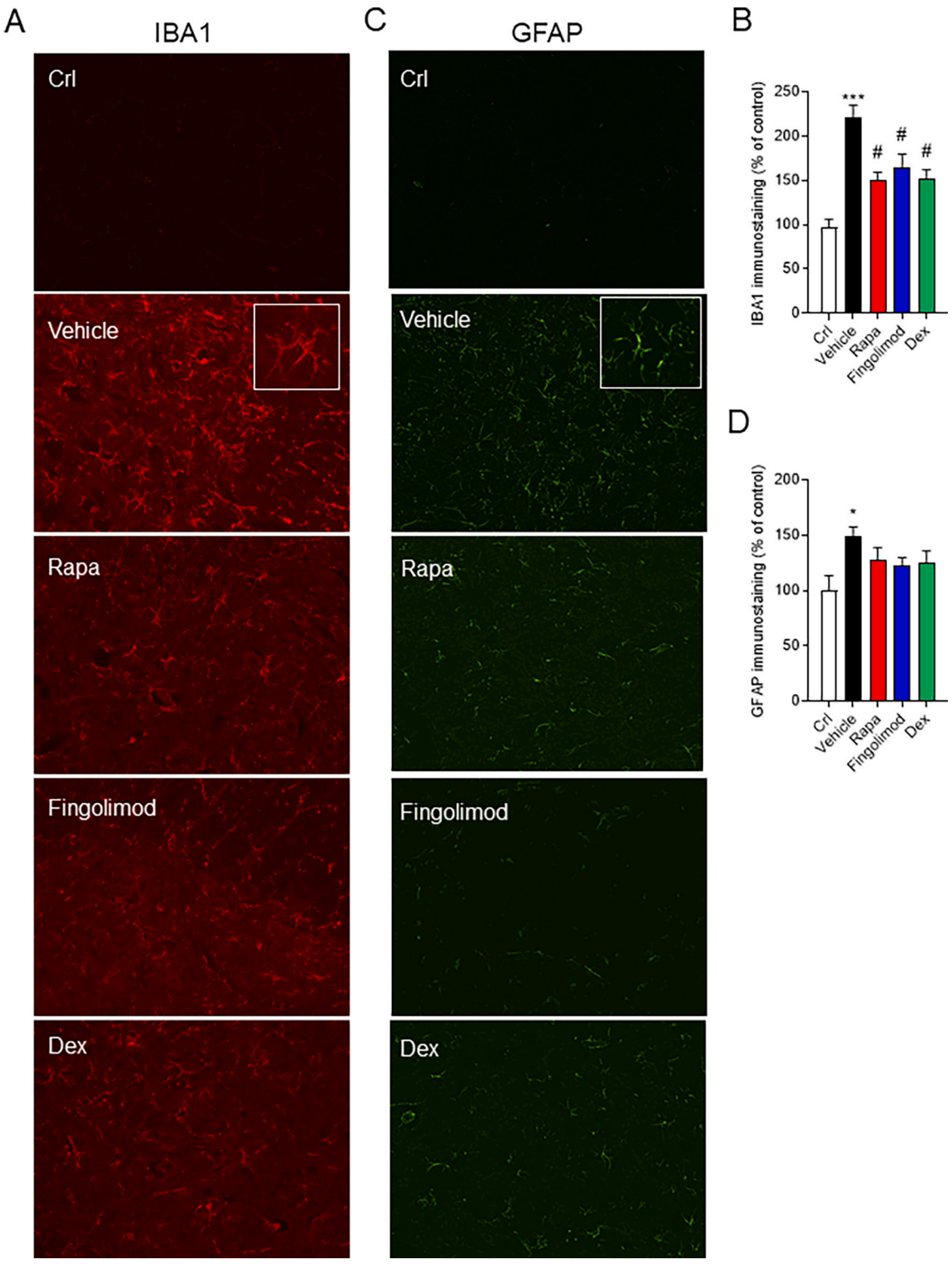

Fig. 5. Effects of rapamycin, dexamethasone and fingolimod on innate immunity in PPEAE NOD mice. Representative confocal images and quantitation of immunostaining of microglia (IBA1) (A and B) and astrocytes (GFAP) (C and D) in spinal cord sections of MOG_{35-55}-immunized NOD mice daily oral treated (from day 0 to 30 post-immunization) with rapamycin (1 mg·kg − 1), dexamethasone (0.3 mg·kg − 1) and fingolimod (0.3 mg·kg − 1). In (B) and (D), each column is the mean ± SEM of five mice per group, four sections per mouse (ANOVA plus Tukey's test). *$p < 0.05$, ***$p < 0.001$ vs Crl, #$p < 0.05$ vs Vehicle.

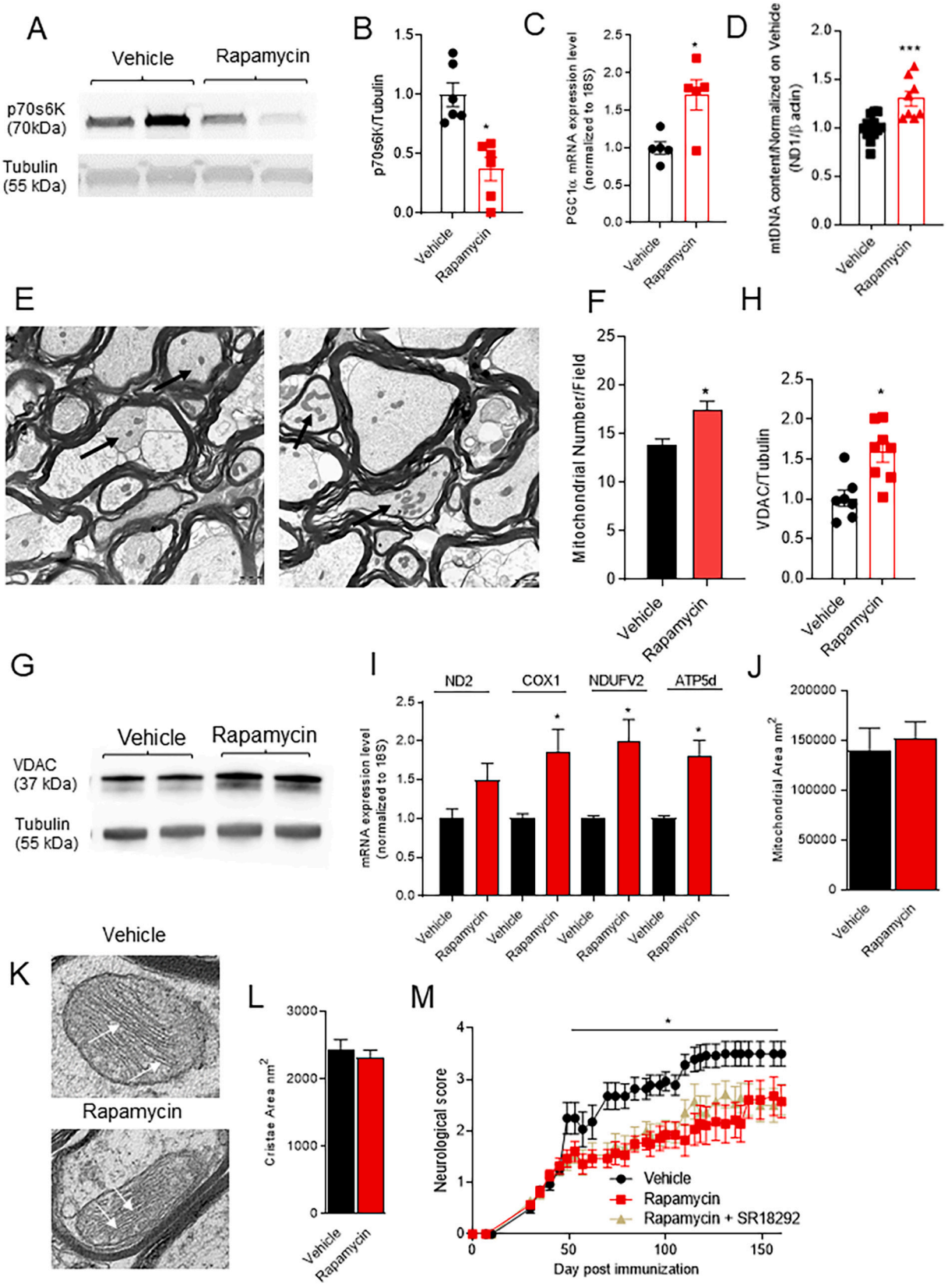

(caption on next page)

Fig. 6. Effects of rapamycin on mitochondrial parameters in the spinal cord of PPEAE NOD mice. Effects of daily oral treatment (from day 0 to 30 post-immunization) with rapamycin (1 mg·kg − 1) on immunized NOD mice**.** Representative (A) and densitometric analysis (B) of p70S6 phosphorylation levels in the spinal cord of immunized NOD mice receiving vehicle or rapamycin (6 mice per group). Expression of PGC1α transcript levels (C) (5 mice per group) and mtDNA content (D) (8 mice per group) in the spinal cord of vehicle- or rapamycin-treated mice. Representative EM images (12.000×) (E) and quantitation (F) of mitochondrial number within axons of spinal cord lateral columns in vehicle- or rapamycin-treated NOD mice. Black arrows indicate axonal mitochondria. Representative (G) and densitometric analysis (H) of VDAC expression levels (7 mice for vehicle and 8 mice for rapamycin) and mRNA levels of mitochondrial (ND2 and COX1) and nuclear (NDUFV2 and ATP5d) respiratory complex subunits (I) (5 mice per group) in the spinal cord of vehicle- or rapamycin-treated mice. Effects of rapamycin treatment on the mitochondrial area are shown (5 sections per animal, 5 mice per group) (J). The mitochondrial cristae area (Mag; 80 K) in the anterior spinal cord columns of vehicle- or rapamycin-treated mice is shown in (K) and quantitated in (L). In (L) 339 and 300 mitochondrial cristae areas belonging to the vehicle- or rapamycin-treated mice were measured. Effects of daily, oral treatment from the day of immunization with rapamycin (1 mg·kg − 1), rapamycin plus SR18292 (both 1 mg·kg − 1) or vehicle on the neurological score in $MOG_{35–55}$- immunized NOD mice ($n = 10$ mice per group) (M). *$p < 0.05$, ***$p < 0.001$ vs vehicle, Student's t-test. In (K) ANOVA plus Tukey's test.

nor fingolimod affected the increase of mitochondria cristae area in the spinal cord lateral column of PEAE NOD mice (Fig. 7G and H).

3.4. Effects of rapamycin on mitochondrial homeostasis in control NOD mice

The impact of rapamycin on mitochondrial homeostasis during EAE progression in NOD mice prompted us to evaluate whether these pharmacological effects exclusively occur within the inflamed spinal cord or are independent of ongoing disease evolution. To answer this question, we exposed healthy NOD mice to the same treatment schedule adopted for those with PEAE and analyzed the same mitochondrial parameters. Supplementary fig. 3A-C shows that the drug was unable to increase PGC1α transcript levels, as well as VDAC expression. Among the different respiratory complex subunits, only COX1 and NDUFV2 showed increased expression levels in rapamycin-treated mice (Supplementary Fig. 3D), and no changes occurred in their spinal cord mtDNA content (Supplementary Fig. 3E). Similarly, axonal mitochondrial area (Supplementary Fig. 3F), as well as cristae area (Supplementary Fig. 3G and H) were unaffected by the drug.

4. Discussion

In the present study, we report the effects of different immunosuppressants in a mouse model of PMS. Overall, we show an inconsistency between the reduction of the autoimmune response and the prevention of disease progression. Specifically, the progression of EAE in NOD mice as well as their survival was unaffected by dexamethasone and fingolimod despite their ability to counteract autoimmunity in the animals. Of note, treatment started on the day of immunization in order to prompt the maximal suppression of the autoimmune response. It is also worth noting that cellular and molecular evidence of immunosuppression occurred even within the mouse spinal cord, thereby indicating substantial prevention of the autoimmune attack on the mouse CNS. We reason that these findings are of particular pathophysiological relevance given that they recapitulate the well-known resistance of MS progression to numerous immunosuppressants otherwise efficacious in the relapsing-remitting form (Baldassari and Fox, 2018). Data suggest, therefore, a significant analogy between the pathological events underlying PEAE and PMS. The peculiarity of this MS mouse model is also suggested by its intrinsic insensitivity to dexamethasone. The latter, indeed, provides significant protection from EAE in a large number of mouse strains (Donia et al., 2010). The insensitivity of PEAE NOD mice to dexamethasone-dependent immunosuppression is also in keeping with the inability of fingolimod to counteract PEAE despite efficient lymphocyte entrapment within lymph nodes. In contrast with this finding, Rothhammer and colleagues reports that fingolimod counteracts disease progression in immunized-NOD mice adopting a daily dose identical to that we used (0.3 $mg{\cdot}kg^{-1}$) but a 40-day i.p. post-treatment (Rothhammer et al., 2017). We demonstrate that the difference in the administration route is not responsible for the different outcomes. Also, we reasoned that the different schedules should not contribute to this discrepancy. Even though we are unable to identify the reason for this apparent inconsistency, it is worth noting that the fingolimod group in the study by Rothhammer and associates is apparently improving before treatment initiation (Rothhammer et al., 2017), suggesting a possible bias in random animal allocation. Of note, our data showing the inefficacy of fingolimod in the PEAE mouse model are consistent with the drug's inefficacy in PMS patients (Smith and Cohen, 2016). Additional studies, however, are needed to clarify the effects of fingolimod in this PEAE model, an issue that appears of particular relevance given the approval of fingolimod analogs siponimod and ozanimod for the treatment of secondary PMS (Krasnov and Kolontareva, 2021; Lamb, 2020).

The present study for the first time reports the ability of rapamycin and everolimus, prototypical immunosuppressants, to counteract disease progression in a mouse model of PMS. The efficacy of two mTOR inhibitors in PEAE NOD mice is of remarkable relevance given the inability of multiple immunosuppressants to counteract disease evolution in this strain. Notably, in the present study, we separately evaluated the effects of two different mTOR inhibitors obtaining similar results. On the one hand, this corroborates the reliability of our findings, and on the other strengthens our conclusion on the efficacy of mTOR inhibition as drugs to counteract PMS. Still, the relevance is further strengthened by the rapamycin's ability to provide the same degree of protection even when a clinically relevant, 30-day post-treatment protocol is adopted. Of course, the identification of the molecular and cellular mechanisms underpinning these pharmacotherapeutic effects might help in understanding PMS pathogenesis and treatment. The analogous qualitative and quantitative suppression of the autoimmune response in NOD mice exposed to dexamethasone, fingolimod and rapamycin suggests however that the latter protects from PEAE through mechanisms unrelated to immunosuppression. In particular, we found that the three drugs reduced at the same extent innate immune response, and similarly prevented adaptive immune response, ruling out that the protective effect of rapamycin is due to a greater effect on immunity of this last compared to dexamethasone or fingolimod. Evidence that the degree of protection with treatments starting at day 0 or 30 (the latter being a time point corresponding to full-blown activation of the autoimmune response) does not differ, further suggests that immunomodulation is not responsible for the therapeutic effects of rapamycin in PEAE mice.

We report a substantial impact of rapamycin on mitochondrial homeostasis in the spinal cord of PEAE mice. Specifically, the drug prompted an increased expression of the master regulator of mitochondriogenesis PGC1α, of several respiratory complex subunits, and also prevented the depletion of mtDNA, an index of mitochondrial content decreasing early during disease progression (Buonvicino et al., 2019). These findings, along with evidence that rapamycin increased expression levels of VDAC, an additional index of mitochondrial content, suggest that support to organelle bioenergetics during PEAE progression is a key mechanism underlying the ability of rapamycin to delay disease evolution. Indeed, a large body of preclinical and clinical evidence points to an impairment of mitochondrial bioenergetics as causative to the initiation and evolution of neurodegeneration in PMS (Blokhin et al., 2008; Campbell and Mahad, 2018; Campbell et al., 2011; Rosenkranz et al., 2021; Witte et al., 2014). In this regard, the ability of the mitochondrial F1Fo-ATP-synthase activator dexpramipexole to delay PEAE

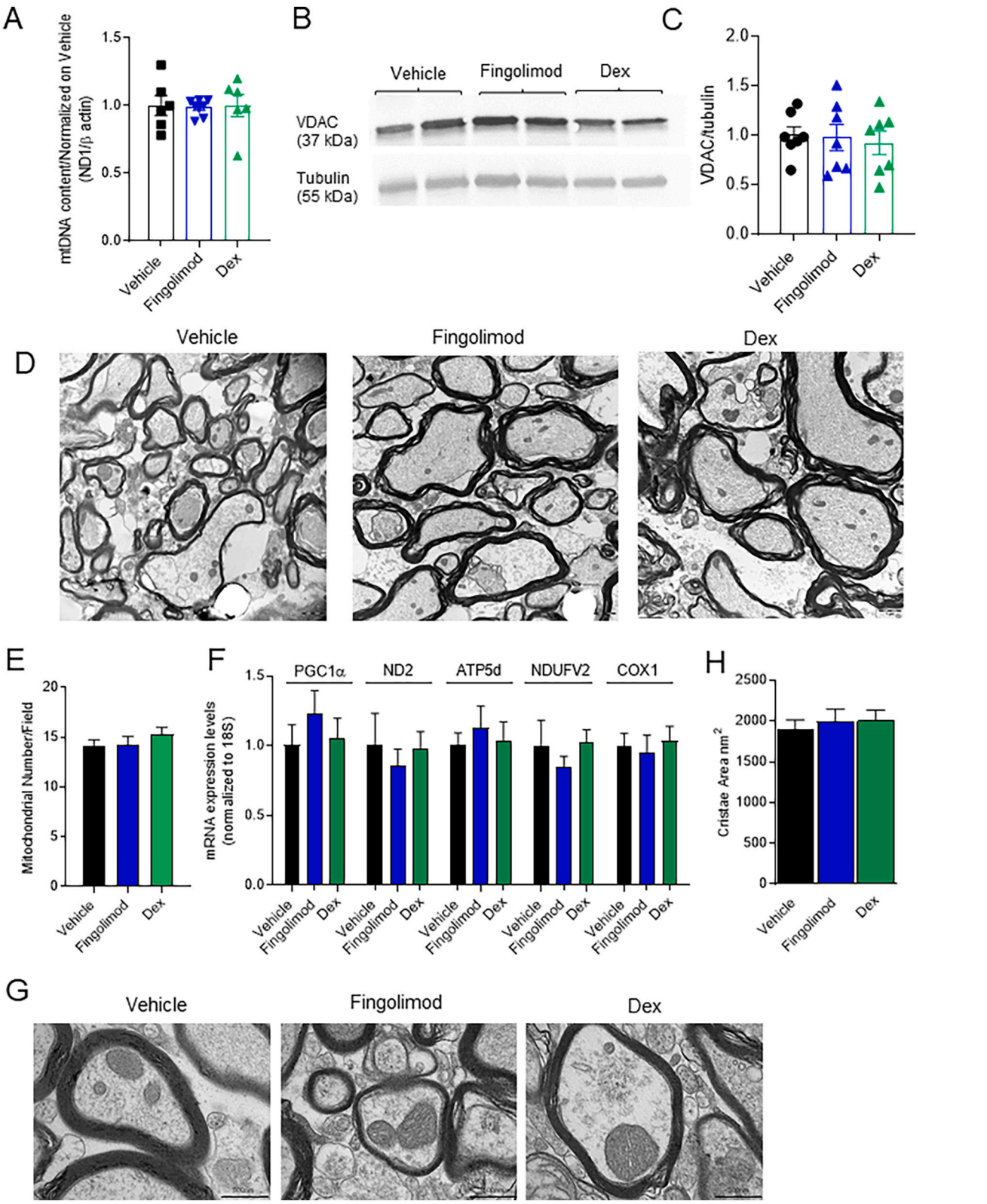

Fig. 7. Effects of fingolimod and dexamethasone on mitochondrial parameters in the spinal cord of NOD-immunized mice. Effects of a daily oral treatment for 30 days with fingolimod (0.3 mg·kg^{-1}) or dexamethasone (0.3 mg·kg^{-1}) on mtDNA content in the spinal cord of NOD-immunized mice (7 mice per group) (A). Representative (B) and densitometric analysis (C) of VDAC expression levels (7 mice per group) in the spinal cord of NOD-immunized mice treated with vehicle, fingolimod, or dexamethasone. Effects of fingolimod or dexamethasone on representative EM images (12.000×) (D) and quantitation (E) of mitochondrial number and on the expression of PGC1α and mitochondrial respiratory complex subunits (F) in the spinal cord of immunized mice treated for 30 days after immunization (5 mice per group). The mitochondrial cristae area (Mag; 80 K) in the anterior spinal cord columns of vehicle-, fingolimod- or dexamethasone-treated mice for 30 days is shown in (G) and quantitated in (H). In (H) 339, 225 and 302 mitochondrial cristae areas belonging to the vehicle-, fingolimod- or dexamethasone-treated mice were measured.

progression in NOD mice (Buonvicino et al., 2020), together with present data showing the inability of dexamethasone and fingolimod to affect disease evolution and mitochondrial homeostasis in these animals, further strengthen the therapeutic implications of the ability of rapamycin to support mitochondrial functioning in PEAE NOD mice. However, the inability of SR18292, a PGC1α inhibitor, to alter the neuroprotective effects of rapamycin suggests that a more complex scenario is responsible for mitochondriogenesis and therapeutic effects induced by rapamycin. In particular, numerous master regulators of mitochondrial biogenesis and shaping such as Pgc1α, Foxo, Nrf2, Hif1α, Opa1, Mfn-1, Mfn-2 and Atp5j2a were been identified, suggesting that several transcriptional regulators could contribute to mitochondrial biogenesis. Admittedly, the possibility that rapamycin-dependent immunosuppression can synergize with the drug's impact on mitochondrial homeostasis cannot be ruled out. Still, rapamycin, fingolimod and dexamethasone were been described as autophagy activators (Wu et al., 2021), further studies are needed to evaluate the possible difference between the three immunosuppressants on this parameter and the subsequent contribution of this mechanism on neuroprotective effects of rapamycin. Rapamycin-dependent neuroprotection, however, is in keeping with prior work showing the drug's ability to reduce neuronal death and mortality in mice null for the Complex I subunit Ndufs4, an animal model of severe neurodegeneration due to failure of mitochondrial bioenergetic (Felici et al., 2017; Johnson et al., 2013). We also show that the effects of rapamycin on mitochondrial homeostasis of PEAE mice can be only in part reproduced in healthy animals. These important findings indicate that pathophysiological events occurring during PEAE sensitize the CNS to the pharmacodynamic effects of rapamycin on mitochondrial homeostasis.

The findings of the present study may have a realistic translational potential. First, they corroborate the relevance of therapeutic approaches sustaining mitochondria, and bioenergetics in general, to PMS therapy (Campbell et al., 2019; Rosenkranz et al., 2021). Accordingly, our recent paper reports that the derangement of mitochondrial homeostasis occurs in the early stage in the NOD mouse model of progressive EAE and that mitochondrial homeostasis is unaffected in a model of relapsing-remitting EAE, underling the central role of mitochondrial during disease progression (Buonvicino et al., 2023). Second, they identify rapamycin as a stand-alone or cotreatment therapeutic approach for PMS therapy. Of note, a single, small trial on the effects of rapamycin in RR-MS patients has been conducted, reporting promising results and a good safety profile (Bagherpour et al., 2018). These clinical findings, along with data from the current study, might expedite the repurposing of rapamycin in the treatment of PMS patients.

In conclusion, the present study furthers our understanding of PEAE in NOD mice as an experimental model of PMS, also highlighting the therapeutic potential of rapamycin and its impact on mitochondrial homeostasis. Confirmatory studies evaluating the pharmacotherapeutic effects of different treatment schedules might corroborate the drug's translational potential to PMS therapy.

Supplementary data to this article can be found online at https://doi.org/10.1016/j.nbd.2023.106387.

Declaration of Competing Interest

Authors declare no conflict of interest.

Data availability

No data was used for the research described in the article.

Acknowledgments

This work was supported by grants from Italian Foundation for Multiple Sclerosis 2014/R/6 and 2022/R-Single/023 (P.I. Alberto Chiarugi), Regione Toscana Rare DiseaseProjects-Heath Projects 2007 and 2009 (P.I. Alberto Chiarugi), AIRC and Fondazione CR Firenze under IG 2017 - ID. 20451 project (P.I. Alberto Chiarugi).

References

Armstrong, J.S., 2007. Mitochondrial medicine: pharmacological targeting of mitochondria in disease. Br. J. Pharmacol. 151 (8), 1154–1165. https://doi.org/10.1038/sj.bjp.0707288.

Bagherpour, B., Salehi, M., Jafari, R., Bagheri, A., Kiani-Esfahani, A., Edalati, M., Kardi, M.T., Shaygannejad, V., 2018. Promising effect of rapamycin on multiple sclerosis. Mult. Scler. Relat. Disord. 26, 40–45. https://doi.org/10.1016/j.msard.2018.08.009.

Baldassari, L.E., Fox, R.J., 2018. Therapeutic advances and challenges in the treatment of progressive multiple sclerosis. Drugs 78 (15), 1549–1566. https://doi.org/10.1007/s40265-018-0984-5.

Basso, A.S., Frenkel, D., Quintana, F.J., Costa-Pinto, F.A., Petrovic-Stojkovic, S., Puckett, L., Monsonego, A., Bar-Shir, A., Engel, Y., Gozin, M., Weiner, H.L., 2008. Reversal of axonal loss and disability in a mouse model of progressive multiple sclerosis. J. Clin. Invest. 118 (4), 1532–1543. https://doi.org/10.1172/JCI33464.

Blokhin, A., Vyshkina, T., Komoly, S., Kalman, B., 2008. Variations in mitochondrial DNA copy numbers in MS brains. J. Mol. Neurosci. 35 (3), 283–287. https://doi.org/10.1007/s12031-008-9115-1.

Buonvicino, D., Urru, M., Muzzi, M., Ranieri, G., Luceri, C., Oteri, C., Lapucci, A., Chiarugi, A., 2018. Trigeminal ganglion transcriptome analysis in 2 rat models of medication-overuse headache reveals coherent and widespread induction of pronociceptive gene expression patterns. Pain 159 (10), 1980–1988. https://doi.org/10.1097/j.pain.0000000000001291.

Buonvicino, D., Ranieri, G., Pratesi, S., Guasti, D., Chiarugi, A., 2019. Neuroimmunological characterization of a mouse model of primary progressive experimental autoimmune encephalomyelitis and effects of immunosuppressive or neuroprotective strategies on disease evolution. Exp. Neurol. 322, 113065 https://doi.org/10.1016/j.expneurol.2019.113065.

Buonvicino, D., Ranieri, G., Pratesi, S., Gerace, E., Muzzi, M., Guasti, D., Tofani, L., Chiarugi, A., 2020. Neuroprotection induced by dexpramipexole delays disease progression in a mouse model of progressive multiple sclerosis. Br. J. Pharmacol. 177 (14), 3342–3356. https://doi.org/10.1111/bph.15058.

Buonvicino, D., Ranieri, G., Chiarugi, A., 2021. Treatment with non-specific HDAC inhibitors administered after disease onset does not delay evolution in a mouse model of progressive multiple sclerosis. Neurosci. 465, 38–45. https://doi.org/10.1016/j.neuroscience.2021.04.002.

Buonvicino, D., Ranieri, G., Guasti, D., Pistolesi, A., La Rocca, A.I., Rapizzi, E., Chiarugi, A., 2023. Early derangement of axonal mitochondria occurs in a mouse model of progressive but not relapsing-remitting multiple sclerosis. Neurobiol. Dis. 178, 106015 https://doi.org/10.1016/j.nbd.2023.106015.

Campbell, G., Mahad, D.J., 2018. Mitochondrial dysfunction and axon degeneration in progressive multiple sclerosis. FEBS Lett. 592 (7), 1113–1121. https://doi.org/10.1002/1873-3468.13013.

Campbell, G.R., Ziabreva, I., Reeve, A.K., Krishnan, K.J., Reynolds, R., Howell, O., Lassmann, H., Turnbull, D.M., Mahad, D.J., 2011. Mitochondrial DNA deletions and neurodegeneration in multiple sclerosis. Ann. Neurol. 69 (3), 481–492. https://doi.org/10.1002/ana.22109.

Campbell, G., Licht-Mayer, S., Mahad, D., 2019. Targeting mitochondria to protect axons in progressive MS. Neurosci. Lett. 710, 134258 https://doi.org/10.1016/j.neulet.2019.05.012.

Cavone, L., Felici, R., Lapucci, A., Buonvicino, D., Pratesi, S., Muzzi, M., Hakiki, B., Maggi, L., Peruzzi, B., Caporale, R., Annunziato, F., Amato, M.P., Chiarugi, A., 2015. Dysregulation of sphingosine 1 phosphate receptor-1 (S1P1) signaling and regulatory lymphocyte-dependent immunosuppression in a model of post-fingolimod MS rebound. Brain Behav. Immun. 50, 78–86. https://doi.org/10.1016/j.bbi.2015.06.019.

Colombo, E., Farina, C., 2021. Lessons from S1P receptor targeting in multiple sclerosis. Pharmacol. Ther. 107971. https://doi.org/10.1016/j.pharmthera.2021.107971.

Curtis, M.J., Alexander, S., Cirino, G., Docherty, J.R., George, C.H., Giembycz, M.A., Hoyer, D., Insel, P.A., Izzo, A.A., Ji, Y., MacEwan, D.J., Sobey, C.G., Stanford, S.C., Teixeira, M.M., Wonnacott, S., Ahluwalia, A., 2018. Experimental design and analysis and their reporting II: updated and simplified guidance for authors and peer reviewers. Br. J. Pharmacol. 175 (7), 987–993. https://doi.org/10.1111/bph.14153.

Donia, M., Mangano, K., Quattrocchi, C., Fagone, P., Signorelli, S., Magro, G., Sfacteria, A., Bendtzen, K., Nicoletti, F., 2010. Specific and strain-independent effects of dexamethasone in the prevention and treatment of experimental autoimmune encephalomyelitis in rodents. Scand. J. Immunol. 72 (5), 396–407. https://doi.org/10.1111/j.1365-3083.2010.02451.x.

Falkowski, S., Woillard, J.B., 2019. Therapeutic drug monitoring of Everolimus in oncology: evidences and perspectives. Ther. Drug Monit. 41 (5), 568–574. https://doi.org/10.1097/FTD.0000000000000628.

Farez, M.F., Quintana, F.J., Gandhi, R., Izquierdo, G., Lucas, M., Weiner, H.L., 2009. Toll-like receptor 2 and poly(ADP-ribose) polymerase 1 promote central nervous system neuroinflammation in progressive EAE. Nat. Immunol. 10 (9), 958–964. https://doi.org/10.1038/ni.1775.

Felici, R., Buonvicino, D., Muzzi, M., Cavone, L., Guasti, D., Lapucci, A., Pratesi, S., De Cesaris, F., Luceri, F., Chiarugi, A., 2017. Post onset, oral rapamycin treatment delays development of mitochondrial encephalopathy only at supramaximal doses. Neuropharmacol. 117, 74–84. https://doi.org/10.1016/j.neuropharm.2017.01.039.

Ferese, R., Lenzi, P., Fulceri, F., Biagioni, F., Fabrizi, C., Gambardella, S., Familiari, P., Frati, A., Limanaqi, F., Fornai, F., 2020. Quantitative ultrastructural morphometry

and gene expression of mTOR-related Mitochondriogenesis within glioblastoma cells. Int. J. Mol. Sci. 21 (13) https://doi.org/10.3390/ijms21134570.
Huntington, N.D., Tomioka, R., Clavarino, C., Chow, A.M., Linares, D., Mana, P., Rossjohn, J., Cachero, T.G., Qian, F., Kalled, S.L., Bernard, C.C., Reid, H.H., 2006. A BAFF antagonist suppresses experimental autoimmune encephalomyelitis by targeting cell-mediated and humoral immune responses. Int. Immunol. 18 (10), 1473–1485. https://doi.org/10.1093/intimm/dxl080.
Ichikawa, M., Koh, C.S., Inoue, A., Tsuyusaki, J., Yamazaki, M., Inaba, Y., Sekiguchi, Y., Itoh, M., Yagita, H., Komiyama, A., 2000. Anti-IL-12 antibody prevents the development and progression of multiple sclerosis-like relapsing–remitting demyelinating disease in NOD mice induced with myelin oligodendrocyte glycoprotein peptide. J. Neuroimmunol. 102 (1), 56–66. https://doi.org/10.1016/s0165-5728(99)00153-8.
Johnson, S.C., Yanos, M.E., Kayser, E.B., Quintana, A., Sangesland, M., Castanza, A., Uhde, L., Hui, J., Wall, V.Z., Gagnidze, A., Oh, K., Wasko, B.M., Ramos, F.J., Palmiter, R.D., Rabinovitch, P.S., Morgan, P.G., Sedensky, M.M., Kaeberlein, M., 2013. mTOR inhibition alleviates mitochondrial disease in a mouse model of Leigh syndrome. Sci. 342 (6165), 1524–1528. https://doi.org/10.1126/science.1244360.
Krasnov, V.S., Kolontareva, Y.M., 2021. Siponimod: a new view at the therapy of secondary progressive multiple sclerosis. Zh. Nevrol. Psikhiatr. Im. S S Korsakova 121 (7), 124–129. https://doi.org/10.17116/jnevro2021121071124 (Siponimod: novyi vzglyad na terapiyu zabolevaniya.).
Lamb, Y.N., 2020. Ozanimod: first approval. Drugs 80 (8), 841–848. https://doi.org/10.1007/s40265-020-01319-7.
Landucci, E., Mazzantini, C., Buonvicino, D., Pellegrini-Giampietro, D.E., Bergonzi, M.C., 2021. Neuroprotective effects of Thymoquinone by the modulation of ER stress and apoptotic pathway in in vitro model of excitotoxicity. Molecules 26 (6). https://doi.org/10.3390/molecules26061592.
Mayo, L., Cunha, A.P., Madi, A., Beynon, V., Yang, Z., Alvarez, J.I., Prat, A., Sobel, R.A., Kobzik, L., Lassmann, H., Quintana, F.J., Weiner, H.L., 2016. IL-10-dependent Tr1 cells attenuate astrocyte activation and ameliorate chronic central nervous system inflammation. Brain 139 (Pt 7), 1939–1957. https://doi.org/10.1093/brain/aww113.
Mix, E., Meyer-Rienecker, H., Hartung, H.P., Zettl, U.K., 2010. Animal models of multiple sclerosis–potentials and limitations. Prog. Neurobiol. 92 (3), 386–404. https://doi.org/10.1016/j.pneurobio.2010.06.005.
Nguyen, L.S., Vautier, M., Allenbach, Y., Zahr, N., Benveniste, O., Funck-Brentano, C., Salem, J.E., 2019. Sirolimus and mTOR inhibitors: a review of side effects and specific management in solid organ transplantation. Drug Saf. 42 (7), 813–825. https://doi.org/10.1007/s40264-019-00810-9.
Pan, Y., Nishida, Y., Wang, M., Verdin, E., 2012. Metabolic regulation, mitochondria and the life-prolonging effect of rapamycin: a mini-review. Gerontol. 58 (6), 524–530. https://doi.org/10.1159/000342204.
Raggi, C., Taddei, M.L., Sacco, E., Navari, N., Correnti, M., Piombanti, B., Pastore, M., Campani, C., Pranzini, E., Iorio, J., Lori, G., Lottini, T., Peano, C., Cibella, J., Lewinska, M., Andersen, J.B., di Tommaso, L., Vigano, L., Di Maira, G., Marra, F., 2021. Mitochondrial oxidative metabolism contributes to a cancer stem cell phenotype in cholangiocarcinoma. J. Hepatol. 74 (6), 1373–1385. https://doi.org/10.1016/j.jhep.2020.12.031.
Rosenkranz, S.C., Shaposhnykov, A.A., Trager, S., Engler, J.B., Witte, M.E., Roth, V., Vieira, V., Paauw, N., Bauer, S., Schwencke-Westphal, C., Schubert, C., Bal, L.C., Schattling, B., Pless, O., van Horssen, J., Freichel, M., Friese, M.A., 2021. Enhancing mitochondrial activity in neurons protects against neurodegeneration in a mouse model of multiple sclerosis. Elife 10. https://doi.org/10.7554/eLife.61798.
Rothhammer, V., Kenison, J.E., Tjon, E., Takenaka, M.C., de Lima, K.A., Borucki, D.M., Chao, C.C., Wilz, A., Blain, M., Healy, L., Antel, J., Quintana, F.J., 2017. Sphingosine 1-phosphate receptor modulation suppresses pathogenic astrocyte activation and chronic progressive CNS inflammation. Proc. Natl. Acad. Sci. U. S. A. 114 (8), 2012–2017. https://doi.org/10.1073/pnas.1615413114.
Rubin Suarez, A., Bilbao Aguirre, I., Fernandez-Castroagudin, J., Pons Minano, J.A., Salcedo Plaza, M., Varo Perez, E., Prieto Castillo, M., 2017. Recommendations of everolimus use in liver transplant. Gastroenterol. Hepatol. 40 (9), 629–640. https://doi.org/10.1016/j.gastrohep.2017.05.008 (Recomendaciones de uso de everolimus en el trasplante hepatico.).
Sedel, F., Bernard, D., Mock, D.M., Tourbah, A., 2016. Targeting demyelination and virtual hypoxia with high-dose biotin as a treatment for progressive multiple sclerosis. Neuropharmacol. 110 (Pt B), 644–653. https://doi.org/10.1016/j.neuropharm.2015.08.028.
Sharabi, K., Lin, H., Tavares, C.D.J., Dominy, J.E., Camporez, J.P., Perry, R.J., Schilling, R., Rines, A.K., Lee, J., Hickey, M., Bennion, M., Palmer, M., Nag, P.P., Bittker, J.A., Perez, J., Jedrychowski, M.P., Ozcan, U., Gygi, S.P., Kamenecka, T.M., Puigserver, P., 2017. Selective chemical inhibition of PGC-1alpha Gluconeogenic activity ameliorates type 2 diabetes. Cell 169 (1), 148–160 e115. https://doi.org/10.1016/j.cell.2017.03.001.
Smith, A.L., Cohen, J.A., 2016. Multiple sclerosis: fingolimod failure in progressive MS INFORMS future trials. Nat. Rev. Neurol. 12 (5), 253–254. https://doi.org/10.1038/nrneurol.2016.37.
Thomson, A.W., Turnquist, H.R., Raimondi, G., 2009. Immunoregulatory functions of mTOR inhibition. Nat. Rev. Immunol. 9 (5), 324–337. https://doi.org/10.1038/nri2546.
Trapp, B.D., Stys, P.K., 2009. Virtual hypoxia and chronic necrosis of demyelinated axons in multiple sclerosis. Lancet Neurol. 8 (3), 280–291. https://doi.org/10.1016/S1474-4422(09)70043-2.
Wang, J., Wang, J., Wang, J., Yang, B., Weng, Q., He, Q., 2019. Targeting microglia and macrophages: a potential treatment strategy for multiple sclerosis. Front. Pharmacol. 10, 286. https://doi.org/10.3389/fphar.2019.00286.
Witte, M.E., Mahad, D.J., Lassmann, H., van Horssen, J., 2014. Mitochondrial dysfunction contributes to neurodegeneration in multiple sclerosis. Trends Mol. Med. 20 (3), 179–187. https://doi.org/10.1016/j.molmed.2013.11.007.
Wu, M.Y., Wang, E.J., Feng, D., Li, M., Ye, R.D., Lu, J.H., 2021. Pharmacological insights into autophagy modulation in autoimmune diseases. Acta Pharm. Sin. B 11 (11), 3364–3378. https://doi.org/10.1016/j.apsb.2021.03.026.
Zheng, X., Boyer, L., Jin, M., Kim, Y., Fan, W., Bardy, C., Berggren, T., Evans, R.M., Gage, F.H., Hunter, T., 2016. Alleviation of neuronal energy deficiency by mTOR inhibition as a treatment for mitochondria-related neurodegeneration. Elife 5. https://doi.org/10.7554/eLife.13378.